Cardiovascular Research (2012) **93**, 141–151
doi:10.1093/cvr/cvr279

Atrial natriuretic peptide enhances microvascular albumin permeability by the caveolae-mediated transcellular pathway

Wen Chen[1], Birgit Gaßner[1], Sebastian Börner[1], Viacheslav O. Nikolaev[2], Nicolas Schlegel[3], Jens Waschke[3], Nadine Steinbronn[4], Ruth Strasser[4], and Michaela Kuhn[1]*

[1]Institute of Physiology, University of Würzburg, Würzburg, Germany; [2]Institute of Pharmacology, University of Würzburg, Würzburg, Germany; [3]Institute of Anatomy, University of Würzburg, Würzburg, Germany; and [4]Heart Center Dresden, Department of Cardiology, University Hospital, Technical University Dresden, Germany

Received 7 April 2011; revised 12 October 2011; accepted 18 October 2011; online publish-ahead-of-print 24 October 2011

Time for primary review: 35 days

Aims Cardiac atrial natriuretic peptide (ANP) participates in the maintenance of arterial blood pressure and intravascular volume homeostasis. The hypovolaemic effects of ANP result from coordinated actions in the kidney and systemic microcirculation. Hence, ANP, via its guanylyl cyclase-A (GC-A) receptor and intracellular cyclic GMP as second messenger, stimulates endothelial albumin permeability. Ultimately, this leads to a shift of plasma fluid into interstitial pools. Here we studied the role of caveolae-mediated transendothelial albumin transport in the hyperpermeability effects of ANP.

Methods and results Intravital microscopy studies of the mouse cremaster microcirculation showed that ANP stimulates the extravasation of fluorescent albumin from post-capillary venules and causes arteriolar vasodilatation. The hyperpermeability effect was prevented in mice with conditional, endothelial deletion of GC-A (EC GC-A KO) or with deleted caveolin-1 (*cav-1*), the caveolae scaffold protein. In contrast, the vasodilating effect was preserved. Concomitantly, the acute hypovolaemic action of ANP was abolished in EC GC-A KO and Cav-1$^{-/-}$ mice. In cultured microvascular rat fat pad and mouse lung endothelial cells, ANP stimulated uptake and transendothelial transport of fluorescent albumin without altering endothelial electrical resistance. The stimulatory effect on albumin uptake was prevented in GC-A- or *cav-1*-deficient pulmonary endothelia. Finally, preparation of caveolin-enriched lipid rafts from mouse lung and western blotting showed that GC-A and cGMP-dependent protein kinase I partly co-localize with Cav-1 in caveolae microdomains.

Conclusion ANP enhances transendothelial caveolae-mediated albumin transport via its GC-A receptor. This ANP-mediated cross-talk between the heart and the microcirculation is critically involved in the regulation of intravascular volume.

Keywords Atrial natriuretic peptide • Microvessel permeability • Caveolin-1

1. Introduction

Cardiac atrial natriuretic peptide (ANP) is an essential physiological, endocrine regulator of arterial blood pressure and intravascular volume.[1] It is secreted from atrial granules into the circulation in response to acute or chronic atrial stretch to act as an antihypertensive and antihypervolaemic factor via its guanylyl cyclase A (GC-A) receptor and intracellular cyclic GMP as second

* Corresponding author: Physiologisches Institut der Universität Würzburg, Röntgenring 9, D-97070 Würzburg, Germany. Tel: +49 931 31 82721; fax: +49 931 31 82741, Email: michaela.kuhn@mail.uni-wuerzburg.de

messenger.[1] Unlike other 'natriuretics' (such as furosemide), which act via the kidneys to reduce interstitial and total body fluid volume with little change in plasma volume, the ANP/GC-A system has important extrarenal, endothelial actions that enable it to reduce plasma volume preferentially.[2] The key mechanism, whereby ANP causes the loss of fluid from the intravascular space, is the increase in endothelial permeability to plasma proteins such as albumin.[2] To prove this concept *in vivo*, we have generated mice with conditional, endothelium-specific deletion of GC-A (EC GC-A KO mice).[3] In these mice, the vasodilating and renal actions of ANP are preserved. Yet, the selective ablation of the endothelial actions of ANP resulted in significant hypervolaemic hypertension, demonstrating that concerted renal and endothelial actions of ANP are essential for the maintenance of intravascular volume homeostasis.[3] However, the post-receptor pathways mediating the stimulation of transvascular albumin transport by ANP are unknown.

The transport of plasma proteins and solutes across the endothelium involves two different routes: one transcellular, via caveolae-mediated vesicular transport, and the other paracellular, via interendothelial junctions.[4] In addition, an intact glycocalyx is part of the primary barrier that retains plasma proteins in the vascular space (reviewed by Curry and Adamson).[5] All these pathways are exquisitely regulated in the resting state and in response to extracellular stimuli and mediators.[4,5] Unfortunately, endothelial cells undergo significant changes in phenotype in culture conditions. For instance, the density of caveolae or the organization of the glycocalyx, endothelial permeability components which could be regulated by ANP, are remarkably different in cultured cells compared with native endothelial cells.[5] Furthermore, cultured endothelial cells, i.e. human umbilical vein endothelial cells, down-regulate specific ANP-modulated signalling pathways (such as cGMP-dependent protein kinase I, cGKI)[6] or up-regulate others (such as the natriuretic peptide clearance receptor). Based on these considerations, the present study was designed mainly to test *in vivo* whether the ANP stimulation of microvascular endothelial albumin permeability involves caveolar transcytosis or paracellular transport pathways. In past studies, we have used the two-tracer method to compare ^{125}I-albumin blood-to-tissue clearances in different mouse tissues. We observed that ANP primarily stimulates vascular permeability in the skin and skeletal muscle.[3,7] These tissues may well serve as dynamic reservoirs of small physiological amounts of intravascular fluid. Based on these observations, in the present study we applied intravital microscopy to study directly the effects of ANP on the extravasation of fluorescently labelled albumin from post-capillary venules within the cremaster muscle of mice. This approach enabled us to distinguish between real increases in microvascular permeability and increased clearance due to changes in microvascular perfusion, especially the effect of an increased number of perfused microvessels after ANP-induced vasodilatation. We used this technique to compare the vasodilating and permeability effects of ANP in wild-type (WT) mice, mice with endothelium-restricted deletion of GC-A,[3] and mice lacking caveolae (Cav-1$^{-/-}$ mice).[8,9] These intravital microscopy studies were combined with measurements of ANP-dependent changes in plasma volume and with *in vitro* studies of albumin uptake in WT, GC-A- or caveolae-deficient cultured microvascular endothelial cells. Together, our observations indicate that the transendothelial vesicular pathway participates in the stimulatory effects of ANP on the albumin permeability of the microcirculation and subsequent changes in plasma volume.

2. Methods

2.1 Genetic mouse models

Mice with selective deletion of the ANP receptor, GC-A, in endothelial cells (EC GC-A KO mice) were generated and genotyped as previously described (Cre/loxP recombination system).[3] Studies were performed with floxed GC-A mice (controls, which retain normal GC-A expression levels) and EC GC-A KO littermates (floxed GC-A mice harbouring the *Tie2-Cre* transgene, which drives the expression of Cre-recombinase in endothelia) in a mixed genetic background (C57BL/6J/129SV). Caveolin-1-deficient (Cav-1$^{-/-}$) mice[8,9] and WT C57BL/6J littermates were from The Jackson Laboratory. Two- to 3-month-old males were used in all studies. All animal investigations conform to the *Guide for the Care and Use of Laboratory Animals* published by the US National Institutes of Health (NIH publication no. 85-23, revised 1996). Experiments were also approved by the animal care committee of the University of Würzburg (approval reference number 54-2531.01-22/07).

2.2 Treatment with *N*-nitro-L-arginine methyl ester

The Cav-1$^{-/-}$ and WT littermates were treated with the nitric oxide/nitric oxide synthase (NOS) inhibitor *N*-nitro-L-arginine methyl ester (L-NAME, 100 mg/kg/day; Sigma), via drinking water for 21 days.[10]

2.3 Intravital microscopy: experimental set-up and calculations

Mice were anaesthetized by an intraperitoneal injection of ketamine (100 mg/kg body weight) and xylazine (10 mg/kg). The depth of anaesthesia was checked by ensuring that noxious pinch stimulation (blunt forceps) of the hindpaw, the forepaw, and the ear did not evoke any motor reflexes. Body temperature was maintained at 37°C. The cremaster muscle was prepared for intravital microscopy on a custom-made stage and continuously superfused with bicarbonate-buffered saline (pH 7.4, 34°C) of the following composition (mM): 138 Na^+, 6 K^+, 2.5 Ca^{2+}, 1.2 Mg^{2+}, 20 HCO_3^-, 1.2 SO_4^{2-}, and 1.2 $H_2PO_4^-$, at a rate of 1.2 mL/min.[11] Thereafter, the animals were transferred onto a microscope stage (Olympus, Hamburg, Germany). At the end of the experiment, the mice were euthanized via intravenous ketamine injection.

To assess microvascular permeability of macromolecules, fluorescein isothiocyanate (FITC)-labelled bovine serum albumin (BSA) or FITC–dextran (MW 150 000; both from Sigma) were dissolved in phosphate-buffered saline at a concentration of 10 mg/mL. The free fluorescent dye in the solution was removed by passing through a size exclusion column. After tail vein injection of 0.1 mL FITC–BSA or FITC–dextran, intravital fluorescence microscopy was performed using a fluorescence filter for FITC for epi-illumination. The microscopic images were recorded by a charge-coupled device camera and transferred to a computer system for off-line evaluation. Topical application of ANP (100 nM; Bachem, Weil am Rhein, Germany) or vehicle was always started 10 min after i.v. administration of FITC–BSA or FITC–dextran and continued for 30 min. Subsequently, histamine (10 μM; Sigma) was superfused for 10 min.

To block caveolae/lipid rafts and thereby transcellular vesicle transport, 1 mM methyl-β-cyclodextrin (MβCD; Sigma) was added to the superfusate.[12] The cremaster muscle was pre-incubated for 15 min, followed by vehicle or ANP superfusion as described above.

Quantitative off-line analysis of the microscopic images was performed with the computer-assisted image analysis system Cell-D (Olympus). The observer was blinded to the treatment and genotype. Changes in microvascular permeability were measured using integrated optical intensity (IOI) as an index.[13] Six interstitial areas, immediately adjacent to post-capillary venules, were randomly selected for IOI analysis. The same pre-selected areas were observed every 10 min.

In a separate series of experiments, we tested the vasodilating effect of topically applied ANP. Measurements were made on pre-capillary arterioles with a diameter of ~25 μm. Only one vessel was studied in each animal. Diameters represent the average of five measurements taken at five locations on each vessel at the same time.[14] Effects of ANP were normalized by expressing data as a percentage of the maximal vasodilatation evoked by topical application of 30 μM sodium nitroprusside (SNP; Sigma) at the end of the experiment.[14]

2.4 Culture of microvascular endothelial cells and cGMP determinations

We performed our *in vitro* studies with two types of microvascular endothelial cells. Rat fad pad endothelial cells (RFPECs; a kind gift from Dr Arie Horowitz, Dartmouth Medical School, Lebanon, NH, USA)[15] were cultured in Dulbecco's modified Eagle's medium containing 10% fetal calf serum.[15] Endothelial cells from peripheral lung tissue of GC-A- or *Cav-1*-deficient and respective control mice (MLECs; murine lung endothelial cells) were isolated and cultured as previously described.[16] We recently reported that RFPECs and WT MLECs express the GC-A receptor and the cGMP-modulated kinase (cGKI).[16] All experiments with RFPECs and MLECs were conducted in mitogen-free, serum-reduced Dulbecco's modified Eagle's medium (0.5% fetal calf serum during 3 h prior to experimentation). The cGMP contents were quantified by radio-immunoassay.[16]

2.5 Determination of fluorescent albumin uptake

Confluent RFPECs and MLECs on glass coverslips were treated with fluorescently tagged albumin (Alexa Fluor 488-labelled BSA; Invitrogen) at 10 μg/mL, plus 0.5 mg/mL unlabelled albumin in phosphate-buffered saline and vehicle or ANP for 30 min.[17] MβCD was used to disrupt caveolae (2 mM, 15 min pre-treatment).[17] Unincorporated probe was removed by rinsing in phosphate-buffered saline. Internalized fluorescent albumin was viewed by confocal microscopy in optical sections mid-way through the cell. Cell nuclei were labelled with 4′,6-diamidino-2-phenyl indole dihydrochloride (DAPI; Thermo Scientific, Dreieich, Germany).[17] Briefly, the monolayer cultures were rinsed and fixed with 4% paraformaldehyde in phosphate-buffered saline; DAPI (1 μg/mL) was added immediately after cell fixation for 10 min. The cells were washed three times with phosphate-buffered saline, and finally mounted on glass slides using Mowiol mounting medium (Sigma). Confocal images were acquired with a laser-scanning confocal microscope (Leica TCS SP5) using diode pumped solid-state UV laser and argon excitation laser line for Alexa 488.

2.6 Permeability assay on permeable supports

RFPECs (100 000 cells per insert) were grown to confluence on gelatin-coated polystyrene filters (Costar Transwell distributed by Corning, Wiesbaden, Germany) in six-well plates over 5 days. After cells were equilibrated in medium with 0.5% fetal calf serum during 3 h, 50 μM FITC–BSA suspended in 100 μL serum-free medium was added to the apical surface. Ten minutes later, 100 nM ANP or 0.125 U/mL thrombin was added apically. FITC–BSA in the basolateral compartment was measured with a fluorescence spectrofluorophotometer after 1, 30, and 60 min. The concentrations were calculated based on standard solutions of FITC–BSA in serum-free medium.

2.7 Transendothelial electrical resistance

Transendothelial electrical resistance was recorded using the electrical impedance system (ECIS 1600R; Applied BioPhysics distributed by Ibidi GmbH, Martinsried, Germany). RFPECs were grown to confluence on gelatine-coated gold microelectrodes. For the experiments, cells were allowed to equilibrate for ~2 h and then either 100 nM ANP or 0.125 U/mL thrombin was added. The effects on transendothelial electrical resistance were recorded during an additional 4 h.

2.8 Preparation of caveolin-enriched lipid raft fractions and western blotting

Freshly isolated mouse lungs were lysed in 2 mL of ice-cold 1% Triton X-100/Mes-buffered saline (MBS) (Mes hydrate 25 mM, pH 6.5, NaCl 0.15 M, and protease inhibitor cocktail) on ice for 1 h.[18] Homogenization was carried out sequentially with a Dounce (Qiagen GmbH, Hilden, Germany) homogenizer (10 strokes), a Polytron (Qiagen GmbH) tissue grinder (three 10 s bursts), and a sonicator (three 20 s bursts). Lysates were mixed with an equal volume of 80% sucrose in MBS (without Triton X-100) and transferred to 14 mm × 89 mm Beckman centrifuge tubes. Three and a half millilitres of 35% sucrose in MBS was layered carefully on the top of the mixture, followed by another 3.5 mL layer of 5% sucrose. Then the sucrose gradient was centrifuged in a SW 41 rotor (Beckman Coulter GmbH, Krefeld, Germany) at 200 000 *g* for 18 h at 4°C. Twelve 1 mL fractions were collected from the top to the bottom of the tube. A light-scattering band at the 5–35% sucrose interface was observed that contained caveolae (fraction 5). Aliquots of all fractions were mixed with Laemmli buffer, denatured at 95°C, and separated by 12% SDS–PAGE. Electrophoresis and immunoblotting were performed as previously described.[16] Antibodies were against GC-A,[16] Cav-1, and cGKI (Cell Signaling Technology, Frankfurt am Main, Germany).

2.9 Acute effects of exogenous ANP on haematocrit

Anaesthetized EC GC-A KO and Cav-$1^{-/-}$ mice and respective control littermates received ANP (500 ng/kg/min, 2.5 μL/kg/h) through a jugular catheter via a microinfusion pump.[3] Haematocrit was measured before and at 30 min of infusion. The conditions of anaesthesia, control of anaesthesia, and method of euthanasia as described for intravital microscopy experiments.

2.10 Statistics

Results are presented as the means ± SEM. Comparisons within groups were performed using ANOVA and Wilcoxon matched pairs test. Data between groups were compared by ANOVA followed by non-parametric Mann–Whitney *U* test, with $P < 0.05$ considered significant.

3. Results

3.1 ANP enhances endothelial albumin permeability of the cremaster microcirculation via the endothelial GC-A receptor

Our first series of *in vivo* experiments aimed to study the vasodilating and permeability effects of ANP in the microcirculation of the mouse cremaster. As shown in *Figure 1A*, topical application of ANP (100 nM) induced a rapid increase in diameter of pre-capillary arterioles, which amounted to 36 ± 4% of maximal dilatation caused by SNP. This vasodilating effect of ANP was not different in control and EC GC-A KO mice. In a separate series of experiments, we studied effects of ANP on FITC–BSA extravasation from post-capillary venules (20–40 μm diameter). As shown in *Figure 1B*, only very subtle increases in interstitial fluorescence intensity were observed during the 30 min superfusion of the cremaster preparation with bicarbonate-buffered saline (vehicle), indicating that the basal leakiness of the microvasculature to albumin was very low. In control mice, topical application of ANP (continuous superfusion with 100 nM ANP, 30 min) led to a mild, progressive increase in interstitial fluorescence intensity, indicating significantly increased microvascular permeability to albumin (*Figure 1B*). On average, baseline interstitial

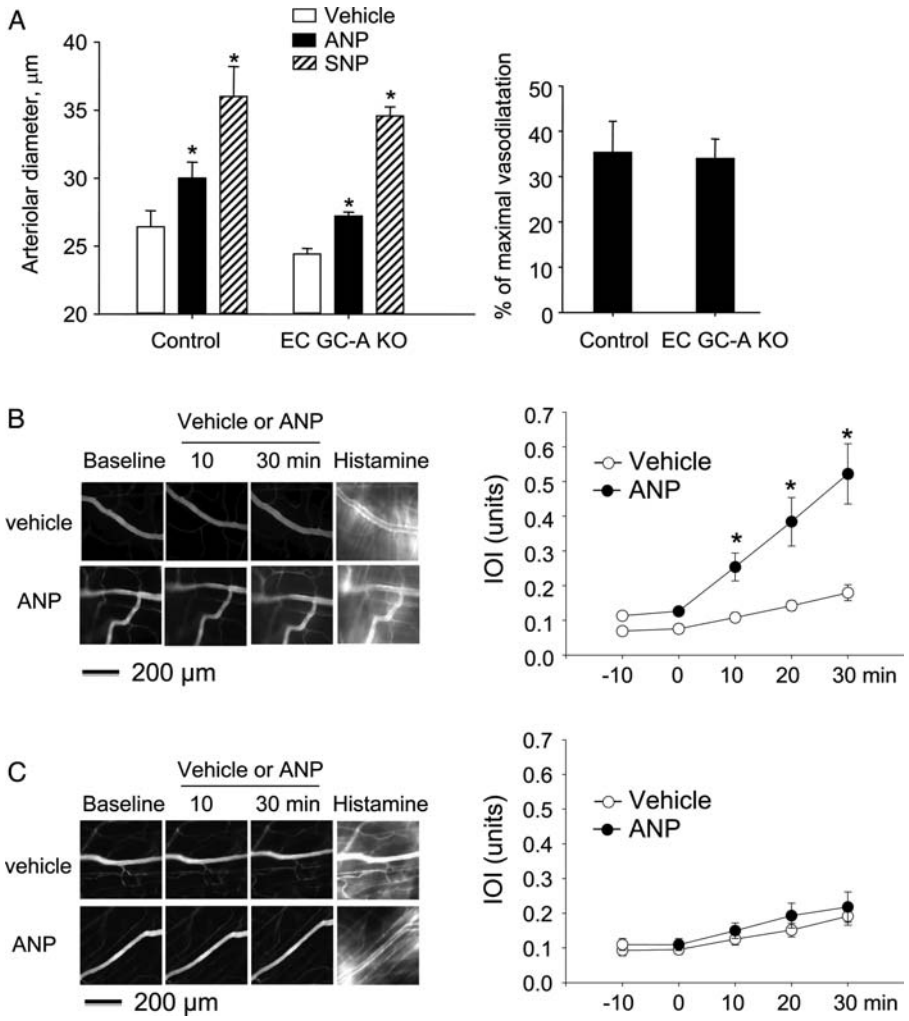

Figure 1 Endothelium-restricted disruption of GC-A preserves the vasodilating but prevents the permeability actions of ANP in the mouse cremaster microcirculation. (*A*) Effect of ANP (100 nM) and SNP (30 μM) on arteriolar diameters in control and EC GC-A KO mice. Left, absolute changes in vessel diameter; right, the effect of ANP is expressed as a percentage of the maximal vasodilatation evoked by subsequent topical application of SNP. (*B* and *C*) Time course of changes in net integrated optical intensity (IOI; an index of permeability) during 30 min of continuous local ANP (100 nM) or vehicle superfusion in control mice (*B*) and in mice with conditional, endothelial GC-A deletion (EC GC-A KO; *C*; $n = 6$ mice per genotype and treatment; $^*P < 0.05$ vs. vehicle). As shown in the original photographs, the hyperpermeability effects of histamine are much greater than the effects of ANP.

fluorescence (IOI) was enhanced by 4.6 ± 0.7-fold at 30 min of ANP superfusion. In EC GC-A KO mice, the stimulatory effect of ANP on FITC–BSA extravasation was abolished (*Figure 1C*). The inflammatory stimulus, histamine (10 μM, superfused for 10 min after vehicle or ANP), provoked immediate, drastic increases in FITC–BSA extravasation which did not differ between control and EC GC-A KO littermates. At 5 min of histamine superfusion, IOI was increased by 7.5 ± 0.6- vs. 6.9 ± 1.1-fold [in arbitrary units: control mice, 0.07 ± 0.01 (baseline) and 0.52 ± 0.05 (histamine; $P < 0.05$ vs. ANP); EC GC-A KO mice, 0.09 ± 0.01 (baseline) and 0.62 ± 0.05 (histamine; $P < 0.05$ vs. ANP)]. At 10 min of continuous histamine superfusion, the effect was slightly reversed (increases in baseline interstitial fluorescence of 6.5 ± 0.7- vs. 5.8 ± 0.8-fold in control and KO mice, respectively). The effects of histamine were similar in vehicle- compared with ANP-treated control tissues (increases in interstitial fluorescence of 7.5 ± 0.6- vs. 8.1 ± 0.1-fold in vehicle vs. ANP-superfused control mice).

Next we tested in control mice the effects of ANP on microvascular permeability for dextran, another high-molecular mass agent. As demonstrated in *Figure 2*, ANP (100 nM, superfused for 40 min) did not enhance FITC–dextran extravasation. In contrast, histamine (10 μM, superfused for 10 min) provoked marked increases in interstitial deposition of FITC–dextran both after vehicle and after ANP superfusion (by 6.8 ± 1.9- vs. 6.4 ± 1.6-fold, respectively; *Figure 2*).

We conclude that ANP, via its endothelial GC-A receptor, increases the transvascular transport of albumin between the blood and interstitial compartment of the cremaster muscle. This permeability effect is independent from the vasodilating action of ANP, is selective for albumin, and is milder than the effect of the inflammatory stimulus, histamine.

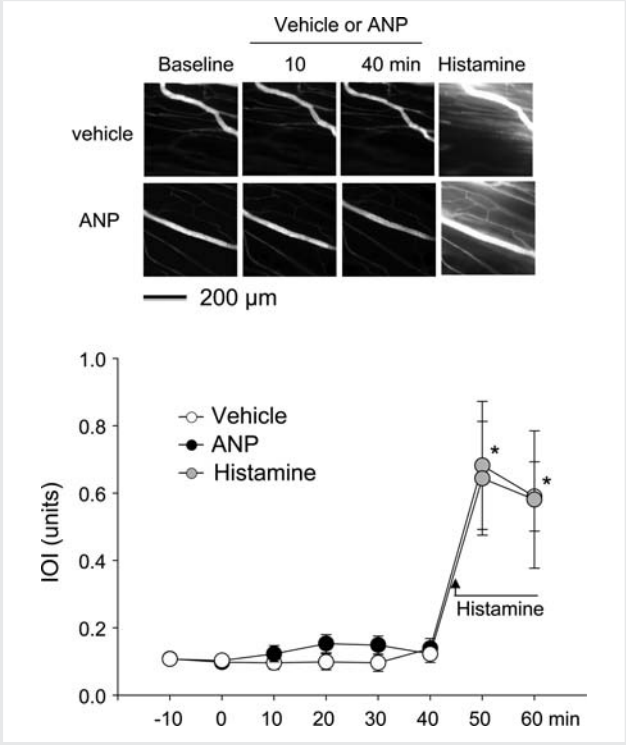

Figure 2 ANP, in contrast to histamine, does not stimulate the extravasation of FITC–dextran within the cremaster microcirculation. Net IOI (an index of permeability) was evaluated during 40 min of continuous local vehicle (saline) or ANP (100 nM) superfusion. Thereafter, histamine (10 μM) was superfused for an additional 10 min ($n = 5$ mice per treatment; $^*P < 0.05$ vs. vehicle).

3.2 ANP induces albumin endocytosis and transcytosis in cultured RFPECs

To differenciate between paracellular and transcellular pathways of albumin transport *in vitro*, the permeability responses to ANP were studied in spontaneously immortalized, well-characterized cultured microvascular endothelial cells from rat epididymal fat pad capillaries (RFPECs).[15] As shown in *Figure 3A*, ANP (10 min incubation) markedly increased the intracellular cGMP content of RFPECs in a concentration-dependent manner, demonstrating expression of the GC-A receptor. We first addressed the possibility that ANP/GC-A activation stimulates endocytosis of albumin, the initial step in albumin transport via transcytosis.[17] As shown in *Figure 3B*, fluorescence, quantified as pixel intensity per cell using confocal microscopy, showed that ANP (10 and 100 nM, 30 min) significantly increased Alexa 488–albumin uptake by RFPECs. Disruption of caveolae by pre-treatment with methyl-β-cyclodextrin (2 mM MβCD for 15 min)[17] prevented the ANP-dependent increase in albumin uptake (*Figure 3B*). Paralleling these responses, ANP enhanced transendothelial, apical-to-basolateral transport of FITC–BSA by RFPECs seeded on permeable filters (*Figure 3C*). To determine whether increased transendothelial albumin flux was the result of opening of interendothelial junctions, we measured changes in transendothelial electrical resistance. Incubation of RFPECs with 100 nM ANP did not alter transendothelial electrical resistance (*Figure 3D*), indicating preservation of paracellular junctions. In comparison, thrombin (0.125 U/mL), which is known to impair the endothelial barrier severely, led to a marked increase in transendothelial FITC–albumin flux (*Figure 3C*) and decreased transendothelial electrical resistance by 80% from baseline (*Figure 3D*). Together, these data indicate that ANP stimulates endocytosis and transcellular transport of albumin by RFPECs. In contrast to thrombin, this occurs without marked opening of interendothelial junctions.

3.3 ANP stimulates caveolae-dependent albumin endocytosis in MLECs

To further investigate whether intact caveolae are required for ANP/GC-A/cGMP-stimulated endothelial albumin endocytosis, we performed experiments with primary cultured microvascular lung endothelial cells (MLECs) isolated from WT, GC-A- or Cav-1-deficient (Cav-$1^{-/-}$) mice. Studies in Cav-$1^{-/-}$ mice have demonstrated the absence of endothelial caveolae and defective transcellular transport of albumin.[8,9] As shown in *Figure 4A*, ANP (10 min incubation) markedly increased intracellular cGMP content in WT MLECs in a concentration-dependent manner. These cGMP responses to ANP were abolished in GC-A-deficient MLECs, but were only slightly and not significantly attenuated in Cav-1-deficient MLECs. At the maximal concentration tested, ANP (1 μM) increased basal cGMP content by 14 ± 3-fold in WT and by 8 ± 1.2-fold in Cav-1-deficient MLECs. Fluorescence, quantified as pixel intensity per cell using confocal microscopy, showed that ANP (10 and 100 nM) induced significant increases in Alexa 488–albumin uptake by WT MLECs (*Figure 5A*). Again, pre-treatment with MβCD (2 mM for 15 min)[17] prevented the ANP-dependent increase in albumin uptake (*Figure 5A*). Furthermore, these stimulatory effects on albumin endocytosis were abolished in GC-A-deficient (*Figure 5B*) or Cav-1-deficient MLECs (*Figure 5C*), corroborating the notion that intact caveolae were required for this endothelial response to ANP/GC-A stimulation. Unfortunately, we could not complement these uptake studies with studies of transendothelial albumin transport. MLECs cultured on permeable supports exhibited a high baseline transendothelial leackage of FITC–BSA, which was not further stimulated by ANP or thrombin.

3.4 The GC-A receptor and its downstream signalling protein, cGKI, are localized in caveolae

To study whether the GC-A receptor is located in caveolae microdomains, Cav-1-rich lipid rafts were purified from murine peripheral lung tissue. As shown in *Figure 4B*, western blotting of membrane fractions demonstrated that a subpopulation of GC-A receptors is indeed located in caveolae, together with Cav-1 as the signature protein of endothelial caveolae (in fraction 5).[8,9] However, a significant amount of GC-A was also detected in other fractions (fractions 8–12). The same distribution was observed for cGKI, a downstream target of GC-A/cGMP.

3.5 Microvascular permeability responses to ANP are abolished in Cav-$1^{-/-}$ mice or by topical superfusion of methyl-β-cyclodextrin

We used Cav-$1^{-/-}$ mice to study whether caveolae are involved in the acute effects of ANP on microvascular albumin permeability and

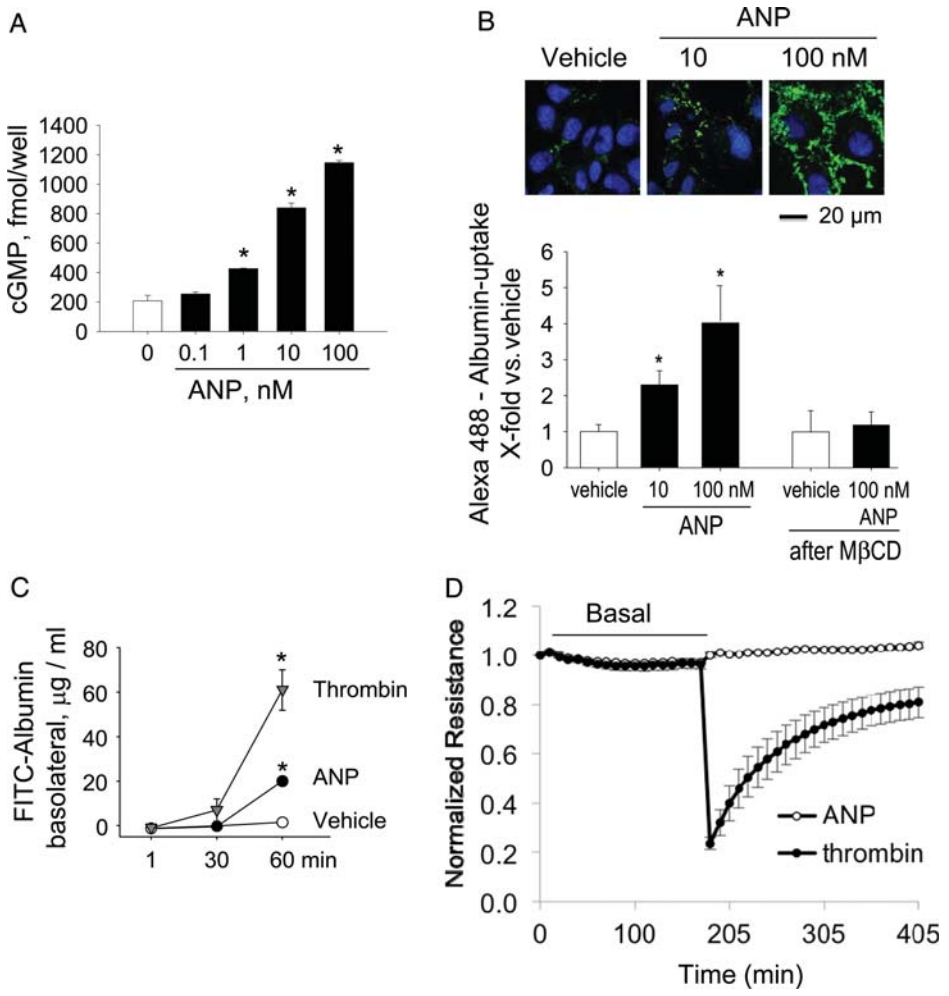

Figure 3 ANP increases cGMP content and stimulates endocytosis and transcellular transport of albumin in microvascular rat fat pad endothelial cells (RFPECs). Effect of ANP on cyclic GMP content (*A*), uptake of Alexa 488-labelled albumin (*B*), transendothelial FITC–BSA permeability (*C*), and TER (*D*). In (*B*), ANP effects were abolished after pre-treatment of RFPECs with MβCD (2 mM, 15 min). In (*C* and *D*), thrombin was used for comparison. (*B*) Confocal images showing ANP-induced concentration-dependent increases in the uptake of Alexa 488-labelled albumin (green). The nucleus (blue) was stained with DAPI. Results are typical of three to four experiments. $^{*}P < 0.05$ compared with vehicle.

intravascular fluid volume. Several groups have shown that, despite the loss of endothelial caveolae, Cav-$1^{-/-}$ mice show marked increases in microvascular paracellular albumin permeability, which is partly due to constitutive activation of endothelial NOS.[19] Treatment with L-NAME (a well-established NOS inhibitor) rescued the microvascular hyperpermeability phenotype of Cav-$1^{-/-}$ mice.[19] Hence, to reverse basal paracellular hyperpermeability and to examine whether absence of caveolae alters the microcirculatory permeability effects of ANP, Cav-$1^{-/-}$ and respective WT mice were treated with L-NAME (100 mg/kg/day, 3 weeks) prior to all experiments. As shown in *Figure 6A*, topical application of ANP (100 nM) once more induced a rapid increase in diameter of pre-capillary arterioles, which amounted to 44 ± 7% of the maximal dilatation caused by SNP. This vasodilating effect of ANP was not different in WT and Cav-$1^{-/-}$ mice. In WT mice, topical superfusion of the cremaster muscle with ANP (100 nM, 30 min) significantly stimulated FITC–BSA extravasation (*Figure 6B*). In Cav-$1^{-/-}$ mice, the basal extravasation of FITC–BSA (during saline superfusion) was slightly higher compared with WT mice (*Figure 6C*); however, the permeability responses to ANP were completely abolished (*Figure 6C*). Note that the rate of FITC–BSA extravasation during ANP superfusion was even lower, as observed during vehicle superfusion. The effects of histamine (10 µM, 10 min) were similar in WT and Cav-$1^{-/-}$ mice (6.6 ± 0.9- and 6.2 ± 1.2-fold increases in baseline interstitial fluorescence) and again were not altered by ANP pre-treatment.

To block caveolae/lipid rafts and thereby transcellular vesicle transport in an acute fashion, in a separate series of experiments with WT mice 1 mM MβCD was added to the superfusate. The cremaster muscle was pre-incubated for 15 min, followed by vehicle or ANP treatment.[12] Unexpectedly, topical application of MβCD itself resulted in significantly increased baseline vascular permeability. As depicted in Supplementary material online, *Figure S1*, significant increases in interstitial fluorescence intensity were observed during the 30 min superfusion of the cremaster preparation with vehicle (after MβCD). ANP had no additional effect on FITC–BSA extravasation (see Supplementary material online, *Figure S1*). In fact, the rate of

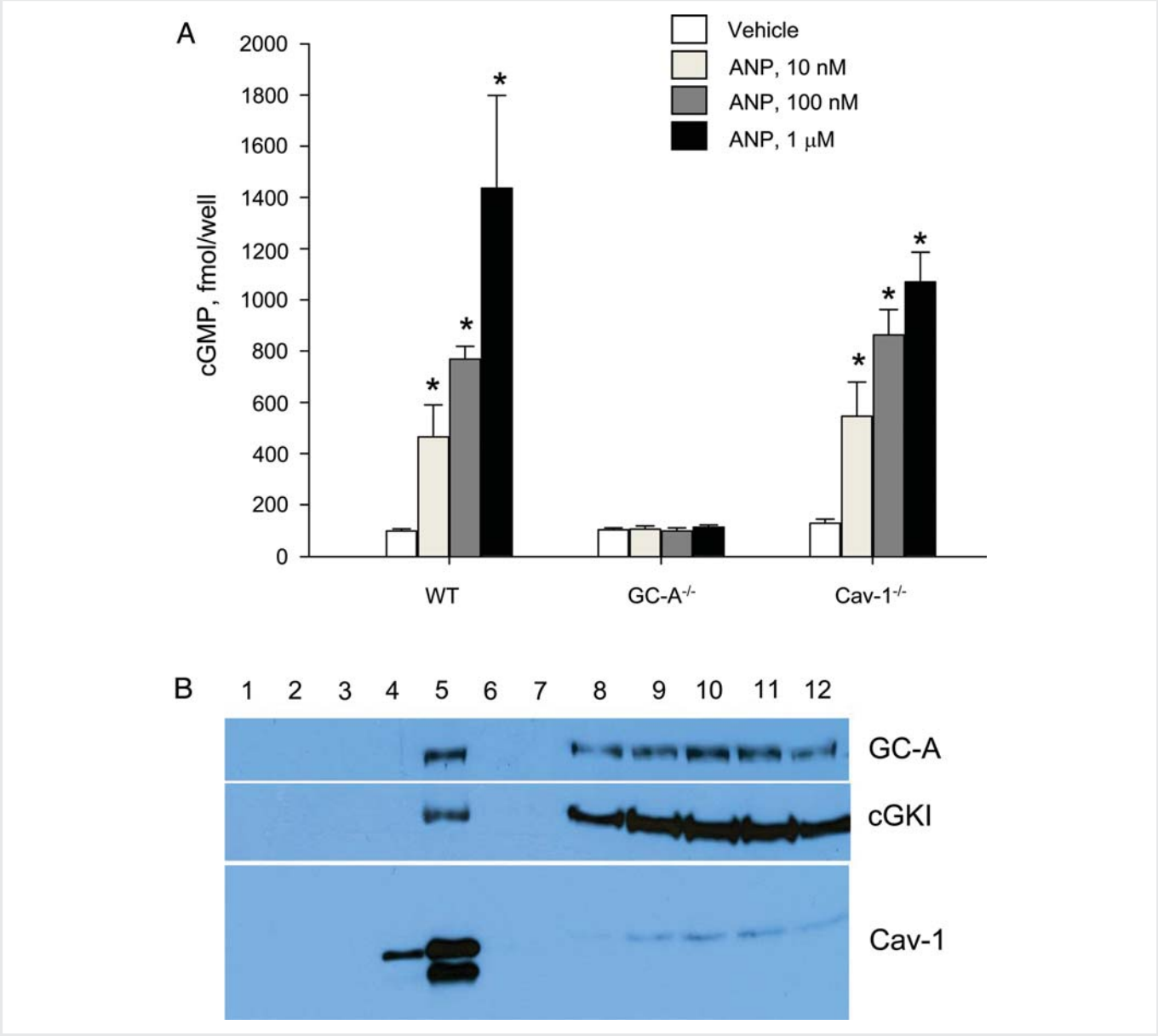

Figure 4 Murine microvascular lung endothelial cells (MLECs) express GC-A receptors, a subpopulation being present in caveolin-enriched lipid rafts. (*A*) Effect of ANP on intracellular cyclic GMP content. ANP increases cGMP in WT but not in GC-A-deficient MLECs. In Cav-1-deficient MLECs, the maximal cGMP responses are slightly but not significantly diminished. (*B*) Peripheral lung tissues were homogenized and subfractionated to isolate light buoyant density membranes (rafts). Western blotting demonstrates the localization of GC-A and cGKI in caveolin-enriched lipid rafts (fraction 5). Immunoblots are representative of three separate experiments.

FITC–BSA extravasation during ANP superfusion was even lower, as observed during vehicle superfusion.

3.6 The acute hypovolaemic responses to ANP are abolished in EC GC-A KO and Cav-1$^{-/-}$ mice

Finally, to study the contribution of endothelial caveolae-mediated albumin transcytosis to the acute hypovolaemic action of ANP, we tested the effect of intravenous ANP administration (500 ng/kg/min, 30 min) on haematocrit. Many previous studies have demonstrated that changes in this parameter in response to ANP reflect acute changes in intravascular fluid volume.[3,20] First, we studied the responses of EC GC-A KO mice and littermate control animals. Infusion of ANP in control mice caused a significant increase in haematocrit by $14 \pm 0.6\%$ ($n = 6$; $P < 0.05$). Taking the average plasma volume of a 30 g mouse as 1530 μL,[3,7] the increase in haematocrit after ANP corresponded to a mean loss of 198 μL fluid from the intravascular to the interstitial space. Similar effects of ANP have been reported in many other studies.[3,7,20] Infusion of ANP failed to increase, and surprisingly, even diminished haematocrit in EC GC-A KO mice by $5.4 \pm 0.7\%$ from baseline ($n = 6$; $P < 0.05$), suggesting a paradoxical hypervolaemic effect.

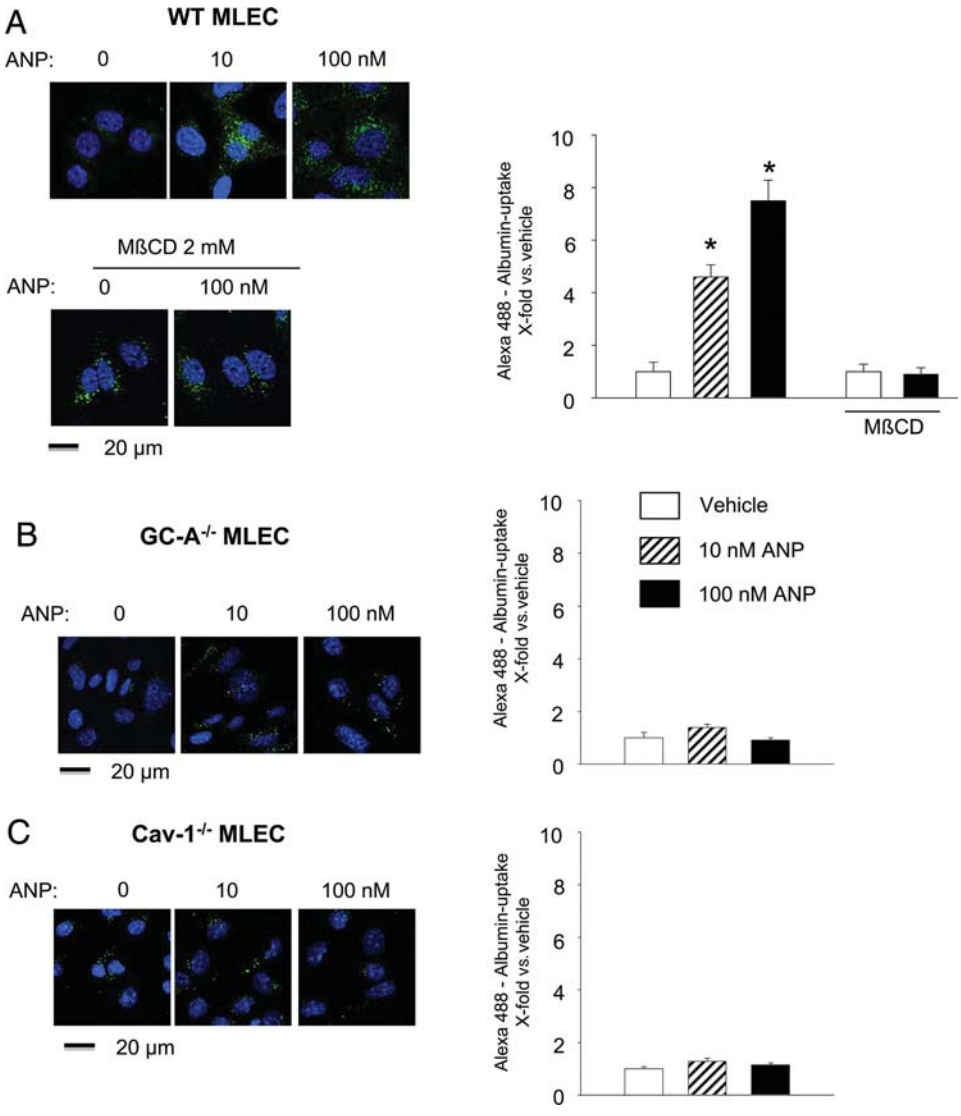

Figure 5 ANP, via GC-A, stimulates caveolae-mediated albumin endocytosis in MLECs. (*A*) Left, confocal images showing the uptake of Alexa 488-labelled albumin (green). The nucleus (blue) was stained with DAPI. Right, fluorescence, quantified as pixel intensity per cell using confocal microscopy, showed that ANP induced concentration-dependent increases in Alexa 488-albumin uptake by WT MLECs. These responses were abolished after pre-treatment of WT MLECs with MβCD (2 mM, 15 min; *A*) as well as in GC-A-deficient (*B*) or in Cav-1-deficient MLECs (*C*). For each genotype, $n = 3–4$. $^*P < 0.05$ compared with vehicle.

To elucidate whether the physiological acute hypovolaemic action of ANP involves caveolae, we studied haematocrit responses in Cav-$1^{-/-}$ and respective WT mice, both pre-treated with L-NAME. Infusion of ANP evoked significant increases in haematocrit of WT mice (by 14.2 ± 1%; $n = 5$, $P < 0.05$). In contrast, ANP infusion had no effect on haematocrit of Cav-$1^{-/-}$ mice ($n = 5$).

4. Discussion

The experiments reported made use of EC GC-A KO and Cav-$1^{-/-}$ mice to investigate the role of endothelial caveolae in the stimulation of physiological permeability by ANP. Intravital microscopy studies of the cremaster muscle microcirculation showed that ANP causes vasodilatation and enhances albumin extravasation. Notably, despite full preservation of the direct vasodilating effect of ANP, the stimulatory effect of ANP on albumin permeability was abolished in EC GC-A KO mice. This permeability effect of ANP is selective for albumin, but not for dextran. It involves endothelial caveolae, because it was absent in mice lacking caveolae (Cav-$1^{-/-}$ mice). Concomitantly, the acute hypovolaemic effects of the hormone were inhibited in EC GC-A KO and Cav-$1^{-/-}$ mice. *In vitro*, ANP stimulated albumin uptake in cultured microvascular rat fat pad and mouse lung endothelia in a GC-A- and Cav-1-dependent manner. Finally, enrichment of caveolae from mouse lungs together with western blot analyses demonstrated that a population of GC-A receptors co-localizes with Cav-1 in caveolae microdomains. Taken together, these data suggest a critical role for caveolae in the ANP-induced mild endothelial hyperpermeability of the systemic microcirculation.

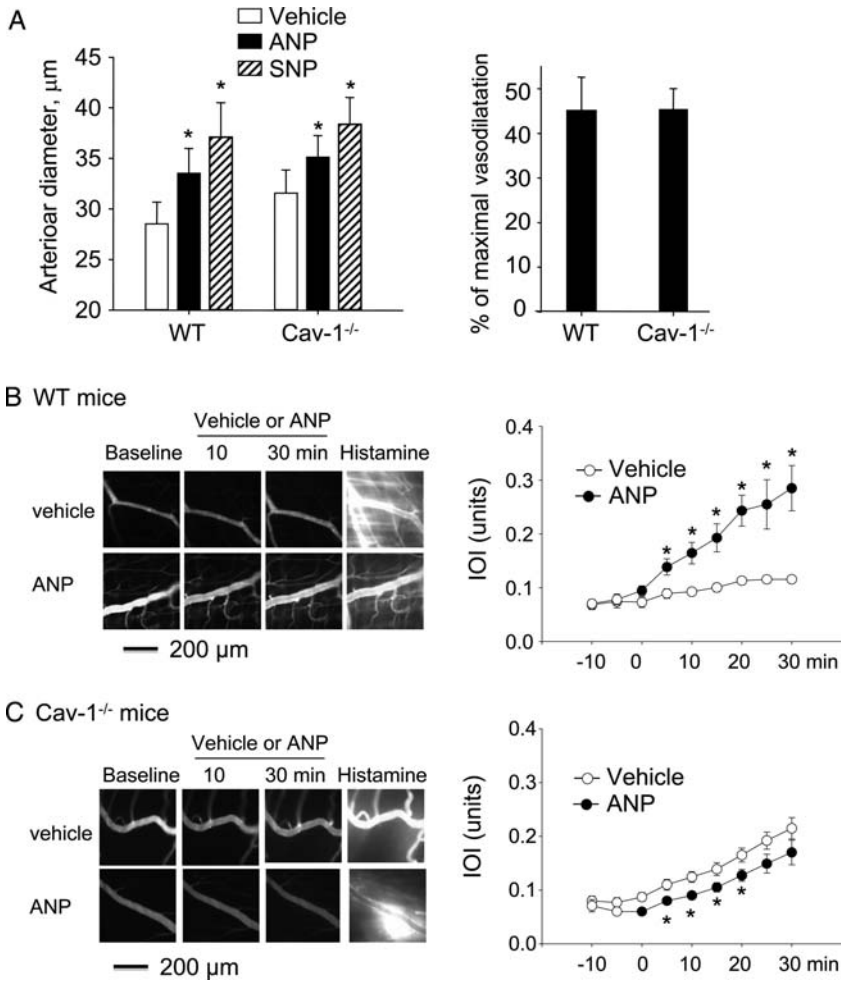

Figure 6 The microvascular hyperpermeability effects of ANP are abolished in Cav-1-deficient mice, while the vasodilatating effects are preserved. (*A*) Effect of ANP (100 nM) and SNP (30 µM) on arteriolar diameters in control and Cav-1$^{-/-}$ mice. Left, absolute changes in vessel diameter; right, the effect of ANP is expressed as a percentage of the maximal vasodilatation evoked by subsequent topical application of SNP. (*B* and *C*) Time course of changes in net IOI during 30 min of continuous local ANP (100 nM) or vehicle superfusion. (*B*) ANP increases FITC–BSA extravasation in control mice. (*C*) The permeability responses to ANP are abolished in mice with deleted *Cav-1* ($n = 8$ mice per genotype and treatment; $^*P < 0.05$ vs. vehicle).

Cav-1$^{-/-}$ mice have contributed a lot to the understanding of caveolin and caveolae; however, these mice exhibit many chronic vascular alterations, such as pathological angiogenesis and paracellular hyperpermeability.[8,19,21] Therefore, we wanted to confirm our observations in this genetic model by a pharmacological approach. To block acutely the caveolae/lipid rafts and thereby transcellular vesicle transport in the mouse microcirculation, the cremaster muscle was locally pre-treated with MβCD.[12] Unexpectedly, after MβCD treatment the baseline albumin extravasation from post-capillary venules was significantly enhanced. ANP treatment, in contrast, had no visible additional effect on microvascular permeability. These results suggest that blockade of caveolae with MβCD inhibits ANP-induced transcytosis, but may itself activate paracellular transport mechanisms, as recognized in Cav-1$^{-/-}$ mice.[19,21] For instance, in cultured epithelial cells, depletion of cell cholesterol with MβCD altered tight junction integrity through the displacement of key junctional proteins (claudins and occludin).[22] Hence, despite all their limitations, Cav-1$^{-/-}$ mice probably represent the best approach to study the role of transendothelial vesicular transport *in vivo*.

Intravital microscopy revealed a decreased number of microvessels in the cremaster muscle of Cav-1$^{-/-}$ compared with WT mice, which is consistant with published studies.[21] However, this anatomical alteration should not influence the results of our *in vivo* experiments with ANP, because we quantified the ANP effects on permeability of single post-capillary venules via fluorescence recordings of interstitial areas immediately adjacent to them.

As caveolae microdomains provide a spatially preferable environment for a variety of receptors, channels, and enzyme systems,[23] we studied whether GC-A is present in this plasma membrane compartment of endothelia, as has been shown for cardiac myocytes.[24] We used peripheral lung tissue to prepare membrane rafts, because our previous studies showed that in this tissue the microvascular endothelial cells are the main source of GC-A. We found that a population of GC-A receptors is indeed located in Cav-1-containing endothelial rafts, suggesting that ANP stimulates caveolae-mediated transcytosis via local GC-A/cGMP signalling; however, a large amount of GC-A protein was also detected in other membrane fractions, outside membrane rafts. Moreover, cGMP responses of

cultured Cav-1 (caveolae)-deficient MLECs to ANP were only attenuated slightly, confirming that a major population of endothelial GC-A receptors is located in other membrane compartments, outside caveolae. This receptor population might mediate other endothelial responses to ANP, such as proliferation and migration,[16] or it may also participate in the regulation of endothelial permeability.

The cellular pathways that link the activation of endothelial GC-A/cGMP to the stimulation of transcellular caveolae-mediated albumin transport remain unknown. Caveolin-1 is the main structural component of endothelial caveolae and regulates endothelial transcytosis.[25] Many molecular aspects of Cav-1-regulated fission and trafficking of caveolae remain unclear. It was shown that *Src* kinase-mediated phosphorylation of Cav-1 on tyrosine 14 stimulates caveolar fission.[25] However, our *in vitro* experiments demonstrated that the levels of Tyr_{14}-phosphorylated Cav-1 following treatment of RFPECs and MLECs with ANP were not changed (immunoblotting; data not shown), suggesting the existence of an independent pathway.

In cultured human fetal macrovascular endothelia (human umbilical vein endothelial cells), ANP/GC-A-mediated cGMP production stimulates phosphodiesterase 2 and thereby lowers cAMP content.[26] As cAMP regulates the stability of intercellular junctions via the Epac/Rap/Rac pathway,[4,26] a decrease in cAMP by ANP could increase paracellular permeability. Other possible actions of GC-A/cGMP are the cGKI-mediated phosphorylation of vasodilator-stimulated phosphoprotein, a protein associated with focal adhesion sites and adherens junctions, as well as modifications of the glycocalyx.[6,27] Although the functional relevance of these ANP/GC-A/cGMP-driven signalling pathways in the microvascular systemic endothelium *in vivo* has not been demonstrated, we cannot rule out the possibility that ANP modulates additional endothelial components contributing to the observed increases in microcirculatory permeability.

Beyond the physiological mild permeability-increasing (volume-regulating) effects on quiescent endothelial cells, ANP has been shown to exert barrier-protecting actions on an inflammation-activated endothelium. The peptide lowered endothelial stress fibre formation and paracellular leakage *in vitro* induced by pro-inflammatory stimuli, such as by hypoxia,[28] lipopolysaccharide,[29] tumour necrosis factor-α, or histamine.[30] Up to now, a single study has validated these observations *in vivo*, demonstrating that exogenous ANP attenuates histamine-induced microvascular FITC–dextran extravasation in rats.[30] In contrast, our intravital microscopy studies did not reveal antagonistic actions of ANP on inflammatory effects of histamine in the mouse cremaster microcirculation. However, as our study was not directed to study possible anti-inflammatory effects of ANP, we tested only a single, very high histamine concentration. Ultimately, the question of whether and when endogenous ANP plays an important pathophysiological role in strengthening the endothelial barrier in inflammatory conditions *in vivo* needs further investigation.

Together with previously published studies,[2,3,7,20] our observations corroborate the notion that concerted renal and endothelial effects of ANP co-operate in the regulation of intravascular volume. To understand this concept, it is important to distinguish the action of a diuretic drug, such as furosemide, from the action of ANP. Trippodo and Barbee demonstrated that the extracellular fluid excreted by the kidney in response to furosemide comes mainly from the interstitial space.[31] In contrast, more than half of the fluid excreted by the kidney in response to ANP comes from the intravascular space.[31] The reason for this difference is that fluid loss, initially from the vascular space during renal water excretion, concentrates the plasma proteins in the vascular space. With furosemide there is no increase in vascular permeability, and the elevated plasma protein oncotic pressure leads to exchanges in fluid from the interstitial space into the vascular space (because the Starling forces governing transvascular fluid exchange shift towards net reabsorption as the plasma protein concentration increases). In this way, significant amounts of fluid can be excreted from the interstitial space by first being reabsorbed into the vascular space from the interstitium and then excreted. This mode of action explains why loop diuretics can be efficiently used for the treatment of oedema. In contrast, as demonstrated here, ANP increases microvascular transendothelial albumin transport at the same time as the diuresis is occuring. There is a shift of the concentrated plasma protein from the vascular to the interstitial space, mainly in skin and skeletal muscle,[7] reduced rate of plasma protein concentration, reduced reabsorption from the extravascular space and preferential loss of fluid from the intravascular space. These co-ordinated renal and endothelial actions of ANP are essential to the chronic maintenance of intravascular volume homeostasis, but also explain the acute hypovolaemic actions of this cardiac hormone.

Supplementary material

Supplementary material is available at *Cardiovascular Research* online.

Conflict of interest: none declared.

Funding

This work was supported by the Deutsche Forschungsgemeinschaft (SFB 688, to M.K. and J.W.).

References

1. Kuhn M. Structure, regulation, and function of mammalian membrane guanylyl cyclase receptors, with a focus on guanylyl cyclase-A. *Circ Res* 2003;**93**:700–709.
2. Curry FR. Atrial natriuretic peptide: an essential physiological regulator of transvascular fluid, protein transport, and plasma volume. *J Clin Invest* 2005;**115**:1458–1461.
3. Sabrane K, Kruse MN, Fabritz L, Zetsche B, Mitko D, Skryabin BV *et al*. Vascular endothelium is critically involved in the hypotensive and hypovolemic actions of atrial natriuretic peptide. *J Clin Invest* 2005;**115**:1666–1674.
4. Komarova Y, Malik AB. Regulation of endothelial permeability via paracellular and transcellular transport pathways. *Annu Rev Physiol* 2010;**72**:463–493.
5. Curry F-RE, Adamson RH. Vascular permeability modulation at the cell, microvessel, or whole organ level: towards closing gaps in our knowledge. *Cardiovasc Res* 2010;**87**:195–197.
6. Smolenski A, Poller W, Walter U, Lohmann SM. Regulation of human endothelial cell focal adhesion sites and migration by cGMP-dependent protein kinase I. *J Biol Chem* 2000;**275**:25723–25732.
7. Curry FR, Rygh CB, Karlsen T, Wiig H, Adamson RH, Clark JF *et al*. Atrial natriuretic peptide modulation of albumin clearance and contrast agent permeability in mouse skeletal muscle and skin: role in regulation of plasma volume. *J Physiol* 2010;**588**:325–339.
8. Drab M, Verkade P, Elger M, Kasper M, Lohn M, Lauterbach B *et al*. Loss of caveolae, vascular dysfunction, and pulmonary defects in caveolin-1 gene-disrupted mice. *Science* 2001;**293**:2449–2452.
9. Schubert W, Frank PG, Razani B, Park DS, Chow CW, Lisanti MP. Caveolae-deficient endothelial cells show defects in the uptake and transport of albumin *in vivo*. *J Biol Chem* 2001;**276**:48619–48622.
10. Sabrane K, Gambaryan S, Brandes RP, Holtwick R, Voss M, Kuhn M. Increased sensitivity to endothelial nitric oxide (NO) contributes to arterial normotension in mice with vascular smooth muscle-selective deletion of the atrial natriuretic peptide (ANP) receptor. *J Biol Chem* 2003;**278**:17963–17968.
11. Siegl D, Koeppen M, Wölfke SE, Pohl U, de Wit C. Myoendothelial coupling is not prominent in arterioles within the mouse cremaster microcirculation in vivo. *Circ Res* 2005;**97**:781–788.
12. Moos MP, Mewburn JD, Kan FW, Ishii S, Abe M, Sakimura K *et al*. Cysteinyl leukotriene 2 receptor-mediated vascular permeability via transendothelial vesicle transport. *FASEB J* 2008;**22**:4352–4362.

13. Hatakeyama T, Pappas PJ, Hobson RW II, Boric MP, Sessa WC, Durán WN. Endothelial nitric oxide synthase regulates microvascular hyperpermeability *in vivo*. *J Physiol* 2006;**574**:275–281.
14. Peyroux J, Beslot F, Claperon N, Fournie-Zaluski MC, Roques BP. Effect of endopeptidase-24.11 inhibitors and C-ANP receptor ligand on responses evoked in arterioles of rat cremaster muscle by atrial natriuretic peptide. *Br J Pharmacol* 1995; **116**:3117–3124.
15. Liu M, Horowitz A. A PDZ-binding motif as a critical determinant of Rho guanine exchange factor function and cell phenotype. *Mol Biol Cell* 2006;**17**:1880–1887.
16. Kuhn M, Völker K, Schwarz K, Carbajo-Lozoya J, Flögel U, Jacoby C *et al*. The natriuretic peptide/guanylyl cyclase-A system functions as a stress-responsive regulator of angiogenesis in mice. *J Clin Invest* 2009;**119**:2019–2030.
17. Hu G, Vogel SM, Schwartz DE, Malik AB, Minshall RD. Intercellular adhesion molecule-1-dependent neutrophil adhesion to endothelial cells induces caveolae-mediated pulmonary vascular hyperpermeability. *Circ Res* 2008;**102**:e120–e131.
18. Song KS, Li S, Okamoto T, Quilliam LA, Sargiacomo M, Lisanti MP. Co-purification and direct interaction of Ras with caveolin, an integral membrane protein of caveolae microdomains. Detergent-free purification of caveolae microdomains. *J Biol Chem* 1996;**271**:9690–9697.
19. Schubert W, Frank PG, Woodman SE, Hyogo H, Cohen DE, Chow CW *et al*. Microvascular hyperpermeability in caveolin-1 (−/−) knock-out mice. Treatment with a specific nitric-oxide synthase inhibitor, L-NAME, restores normal microvascular permeability in Cav-1 null mice. *J Biol Chem* 2002;**277**:40091–40098.
20. Flückiger JP, Waeber B, Matsueda G, Delaloye B, Nussberger J, Brunner HR. Effect of atriopeptin III on hematocrit and volemia of nephrectomized rats. *Am J Physiol* 1986; **251**:H880–H883.
21. Chang SH, Feng D, Nagy JA, Sciuto TE, Dvorak AM, Dvorak HF. Vascular permeability and pathological angiogenesis in caveolin-1-null mice. *Am J Pathol* 2009;**175**: 1768–1776.
22. Lambert D, O'Neill CA, Padfield PJ. Depletion of Caco-2 cell cholesterol disrupts barrier function by altering the detergent solubility and distribution of specific tight-junction proteins. *Biochem J* 2005;**387**:553–560.
23. Simons K, Gerl MJ. Revitalizing membrane rafts: new tools and insights. *Nat Rev Mol Cell Biol* 2010;**11**:688–699.
24. Doyle DD, Ambler SK, Upshaw-Earley J, Bastawrous A, Goings GE, Page E. Type B atrial natriuretic peptide receptor in cardiac myocyte caveolae. *Circ Res* 1997;**81**:86–91.
25. Shajahan AN, Tiruppathi C, Smrcka AV, Malik AB, Minshall RD. $G_{\beta\gamma}$ activation of Src induces caveolae-mediated endocytosis in endothelial cells. *J Biol Chem* 2004;**279**: 48055–48062.
26. Surapisitchat J, Jeon KI, Yan C, Beavo JA. Differential regulation of endothelial cell permeability by cGMP via phosphodiesterases 2 and 3. *Circ Res* 2007;**101**: 811–818.
27. Bruegger D, Jacob M, Rehm M, Loetsch M, Welsch U, Conzen P *et al*. Atrial natriuretic peptide induces shedding of endothelial glycocalyx in coronary vascular bed of guinea pig hearts. *Am J Physiol* 2005;**289**:H1993–H1999.
28. Irwin DC, Tissot van Patot MC, Tucker A, Bowen R. Direct ANP inhibition of hypoxia-induced inflammatory pathways in pulmonary microvascular and macrovascular endothelial monolayers. *Am J Physiol* 2005;**288**:L849–L859.
29. Birukova AA, Xing J, Fu P, Yakubov B, Dubrovskyi O, Fortune JA *et al*. Atrial natriuretic peptide attenuates LPS-induced lung vascular leak: role of PAK1. *Am J Physiol* 2010; **299**:L652–L663.
30. Fürst R, Bubik MF, Bihari P, Mayer BA, Khandoga AG, Hoffmann F *et al*. Atrial natriuretic peptide protects against histamine-induced endothelial barrier dysfunction in vivo. *Mol Pharmacol* 2008;**74**:1–8.
31. Trippodo NC, Barbee RW. Atrial natriuretic factor decreases whole-body capillary absorption in rats. *Am J Physiol* 1987;**252**:R915–R920.